Elsevier Editorial System(tm) for
International Journal of Pharmaceutics
Manuscript Draft

Manuscript Number: IJP-D-18-02374R1

Title: Retentive device for intravesical drug delivery based on water-induced shape memory response of poly(vinyl alcohol): design concept and 4D printing feasibility

Article Type: Research Paper

Section/Category:

Keywords: shape memory polymer; poly(vinyl alcohol); hot melt extrusion; fused deposition modeling; 3D printing; 4D printing; intravesical delivery.

Corresponding Author: Dr. Lucia Zema, Ph.D.

Corresponding Author's Institution: Università degli Studi di Milano

First Author: Alice Melocchi

Order of Authors: Alice Melocchi; Nicoletta Inverardi; Marco Uboldi; Francesco Baldi; Alessandra Maroni; Stefano Pandini; Francesco Briatico-Vangosa; Lucia Zema, Ph.D.; Andrea Gazzaniga

Abstract: The use of shape memory polymers exhibiting water-induced shape recovery at body temperature and water solubility was proposed for the development of indwelling devices for intravesical drug delivery. These could be administered via catheter in a suitable temporary shape, retained in the bladder for a programmed period of time by recovery of the original shape and eliminated with urine following dissolution/erosion. Hot melt extrusion and fused deposition modeling 3D printing were employed as the manufacturing techniques, the latter resulting in 4D printing because of the shape modifications undergone by the printed item over time. Pharmaceutical-grade poly(vinyl alcohol) was selected based on its hot-processability, availability in different molecular weights and on preliminary data showing water-induced shape memory behavior. Specimens having various original and temporary geometries as well as compositions, successfully obtained, were characterized by differential scanning calorimetry and dynamic-mechanical thermal analysis as well as for fluid uptake, mass loss, shape recovery and release behavior. The samples exhibited the desired ability to recover the original shape, consistent in kinetics with the relevant thermo-mechanical properties, and concomitant prolonged release of a tracer. Although preliminary in scope, this study indicated the viability of the proposed approach to the design of retentive intravesical delivery systems.

***Graphical Abstract (for review)**

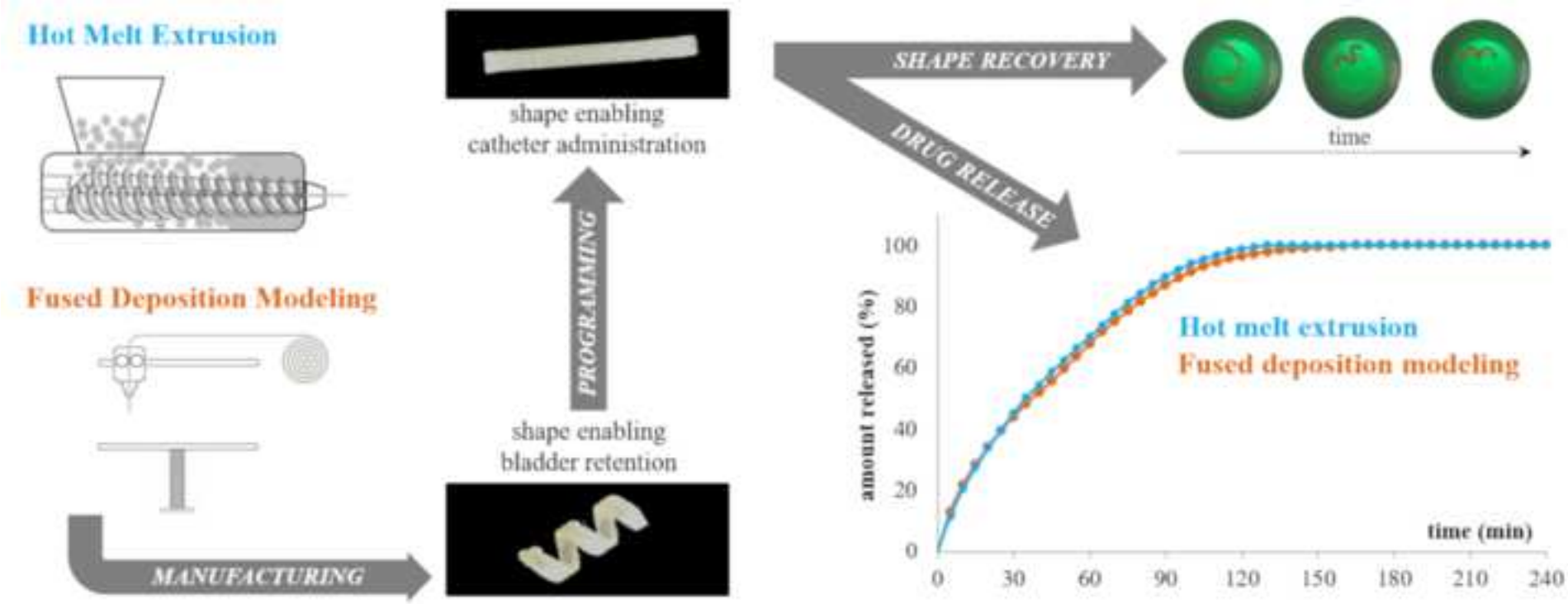

Retentive device for intravesical drug delivery based on water-induced shape memory response of poly(vinyl alcohol): design concept and 4D printing feasibility

A. Melocchi[a1], N. Inverardi[b1], M. Uboldi[a], F. Baldi[b], A. Maroni[a], S. Pandini[b], F. Briatico-Vangosa[c*], L. Zema[a*], A. Gazzaniga[a]

[a]Dipartimento di Scienze Farmaceutiche, Sezione di Tecnologia e Legislazione Farmaceutiche "Maria Edvige Sangalli", Università degli Studi di Milano, Milano, Italy;

[b]Dipartimento di Ingegneria Meccanica e Industriale, Università degli Studi di Brescia, Brescia, Italy;

[c]Dipartimento di Chimica, Materiali e Ingegneria Chimica "G. Natta", Politecnico di Milano, Milano, Italy.

[1]These authors contributed equally to the work.

[*]Corresponding authors: Lucia Zema, telephone: +39 02 50324654, e-mail: lucia.zema@unimi.it, and Francesco Briatico-Vangosa, telephone: +39 02 23993290, e-mail: francesco.briatico@polimi.it

Abstract

The use of shape memory polymers exhibiting water-induced shape recovery at body temperature and water solubility was proposed for the development of indwelling devices for intravesical drug delivery. These could be administered *via* catheter in a suitable temporary shape, retained in the bladder for a programmed period of time by recovery of the original shape and eliminated with urine following dissolution/erosion. Hot melt extrusion and fused deposition modeling 3D printing were employed as the manufacturing techniques, the latter resulting in 4D printing because of the shape modifications undergone by the printed item over time. Pharmaceutical-grade poly(vinyl alcohol) was selected based on its hot-processability, availability in different molecular weights and on preliminary data showing water-induced shape memory behavior. Specimens having various original and temporary geometries as well as compositions, successfully obtained, were characterized by differential scanning calorimetry and dynamic-mechanical thermal analysis as well as for fluid uptake, mass loss, shape recovery and release behavior. The samples exhibited the desired ability to recover the original shape, consistent in kinetics with the relevant thermo-mechanical properties, and concomitant prolonged release of a tracer. Although preliminary in scope, this study indicated the viability of the proposed approach to the design of retentive intravesical delivery systems.

Keywords: shape memory polymer; poly(vinyl alcohol); hot melt extrusion; fused deposition modeling; 3D printing; 4D printing; intravesical delivery.

List of abbreviation

3D: three dimensional

4D: four dimensional

α: angle between the two arms of U- and I-shaped samples during recovery

α_p: angle obtained in the programming phase of shape recovery experiments

CAD: computer-aided design

CFF: caffeine

DSC: differential scanning calorimetry

DMTA: dynamic-mechanical thermal analysis

E': storage modulus

E'_{Troom}: storage modulus at room temperature

E'_{Tdef}: storage modulus at deformation temperature

FDM: fused deposition modeling

FU: fluid uptake

GLY: glycerol

HME: hot melt extrusion

N_{final}: number of windings of helical-shaped samples at the end of recovery

N_0: number of windings of helical-shaped samples before programming

PVA: poly(vinyl alcohol)

RDM: residual dry mass

RI: recovery index

RI_{final}: final recovery index

SMP: shape memory polymer

T_{def}: deformation temperature

T_g: glass transition temperature

T_{room}: room temperature

$t_{10\%}$: time needed to reach 10% of drug release

$t_{90\%}$: time needed to reach 90% of drug release

$t_{RIfinal}$: time needed to reach final recovery index

W_m: mass of the wet sample on withdrawal

W_d: mass of the sample after drying

W_i: initial mass of the sample

1. Introduction

The bladder is a muscle-epithelial sac responsible for the collection of waste substances from the systemic circulation, coming from the kidneys, and their elimination as urinary fluids (GuhaSarkar, and Banerjee, 2010, Hsu et al, 2013, Zacchè et al., 2015). Considering its pivotal role in the homeostasis of the human body, any change in its functionality, even caused by the natural aging process or brought about by the onset of diseases, is necessarily associated with inconveniences of different extent. Vesical diseases, such as atonic and hyperactive bladder, interstitial cystitis and cancer, are widespread in individuals of different age and gender. However, their incidence increases in elderly people, who represent the population segment of developed countries in continuous growth and whose therapeutic treatments have great impact on healthcare expenses. The pharmacological therapy of such pathologies involves both systemic administration, mainly by the oral route, and *in situ* transurethral instillation of different active ingredients. Topical administration of drugs offers several advantages, *e.g.* to reduce the systemic side effects and avoid possible presystemic elimination mainly by the liver (first-pass effect), thus also allowing lower drug strengths to be used. Currently, solutions, suspensions or emulsions containing one or more drugs are instilled into the bladder through a catheter, inserted directly into the urethra of the patient and then clamped off for a pre-determined time period (from few minutes up to at least 1 h for chemotherapy), before being drained or normally excreted after withdrawal of the catheter. In the case the latter is removed immediately after instillation and the patient is asked to keep the solution in the bladder for the longest possible time, the maximum residence time of drugs within the bladder hardly exceeds 2 h, even when fluid intake is avoided. With the aim of counteracting the drug washout, repeated instillations are thus required, and this may entail other complications, such as primarily the onset of infections.

In order to maintain effective concentrations of the bioactive molecules within the bladder, various strategies have been pursued such as the use of bioadhesive liposome- or thermosensitive hydrogel-based formulations (Cima et al., 2014, Farokhzad et al., 2006, Nirmal et al. 2010, Tyagi et al., 2016). One of the most innovative approaches to intravesical delivery is represented by indwelling systems

administered transurethrally *via* catheter, that are designed to remain in the bladder for longer time periods (*e.g.* weeks). This resembles the concept of expandable gastroretentive dosage forms, the original size of which is reduced, *e.g.* by folding, into a carrier system such as a capsule: after administration, the carrier dissolves or opens up in stomach and the unit conveyed recovers a significantly larger spatial encumbrance due to swelling or unfolding processes that prolong its gastric retention time (Klausner et al., 2003). Analogously, bladder retention was obtained through either an increase in the size of the devices (*e.g.* UROS, Situs Corporation) or a change in the relevant geometry after being positioned into the organ (*e.g.* LiRIS, TARIS Biomedical). The success of the indwelling drug delivery systems described so far is still limited due to their poor tolerability, mainly associated with relatively large dimensions, density higher than that of urine and need for a removal procedure at the end of the treatment (Lee and Choy, 2016, Lee and Cima, 2011, Nickel et al., 2012). The idea of a biodegradable indwelling system that would not involve subsequent removal was preliminarily proposed (Tobias et al., 2010). However, the mechanism of retention (*e.g.* based on size increase or on geometry variation) was not clearly defined.

Over the last few years, shape memory polymers (SMPs) have drawn great interest in the area of advanced systems intended for biomedical applications (Behl and Lendlein, 2007, Chan et al., 2016, El Feninat et al., 2002, Lendlein and Langer, 2002, Lendlein et al., 2010, Sokolowski et al., 2007, Yahia, 2015). They belong to smart materials capable of *i)* memorizing a permanent/original shape, *ii)* being fixed, under appropriate temperature conditions and mechanical stress, to a temporary shape and *iii)* being triggered, by an external *stimulus* such as a change in temperature, light, moisture, magnetic field or electrical current, to spontaneously recover the memorized stress-free permanent shape (Liu et al., 2007; Hager et al., 2015; Huang et al., 2010). Microstructural changes of the polymer are responsible for shape fixing and shape recovery, the latter relaxation step being associated with elastic deformation stored during previous manipulation.

In this respect, much attention has been focused on SMP-based devices in which shape changes could be obtained at body temperature. Once introduced into the human body, these would be able to modify

their shape thanks to exposure to 37 °C, thus performing their function. Interestingly, in a particular class of SMPs, shape modifications can be triggered not only by heating but also through contact with water (*i.e.* water-induced shape memory effect). Such SMPs are hydrophilic polymers for which water taken up acts as a plasticizer and reduces the temperature required to activate the shape memory response (Yang et al., 2004). In addition, SMPs characterized by water-induced shape memory behavior and suitable thermoplastic properties could be subjected to hot-processing *via* forming manufacturing techniques, such as hot melt extrusion (HME), injection molding and fused deposition modeling (FDM) 3D printing, which are well-known to yield high versatile geometries, details and sizes of products. Notably, the combined use of 3D printing technologies and SMPs has recently led to the new concept of 4D printing, intended as fabrication *via* 3D printing of items capable of self-transforming after production in terms of morphology, and thus possibly of functionality, in response to an external *stimulus* (Ding et al., 2017, Gao et al., 2016, Lee et al., 2017; Maniruzzamann 2018). As compared with 3D printing, 4D printing involves the use of smart materials and also an advanced design, which has to take account of the original shape, the temporary shape, the transformations undergone by the object to shift from one another and relevant mechanisms. The time frame in which the original shape is recovered represents the 4th dimension. In spite of the huge potential held, major applications of 4D printing in the development of drug delivery systems are yet to come.

Based on such premises, the aim of the present work was to study the possible water-induced shape memory response of specimens fabricated from poly(vinyl alcohol) (PVA) of pharmaceutical grade by means of hot-processing techniques, namely HME and FDM. In particular, PVA was chosen in view of its known suitability for hot-processing and on preliminary results pointing out its water-induced shape memory behavior. Indeed, such a property could advantageously be exploited for the development of intravesical retentive systems, *i.e.* devices suitable for administration *via* catheter in the programmed/temporary shape and for bladder retention following spontaneous recovery of the permanent/original shape. Thanks to its slow interaction with aqueous fluids and related dissolution, it was deemed to hold potential as the main component of an indwelling drug delivery system for

prolonged release, with no need for being removed thanks to its erosion/dissolution over time. Moreover, the release rate could interestingly be tuned by selecting the polymer molecular weight. The feasibility of 4D printing in the manufacturing of such a device was preliminarily evaluated by characterizing the specimens obtained for thermo-mechanical properties, water-induced shape recovery, fluid uptake, mass loss as well as release behavior, using samples containing an analytical tracer.

2. Materials and Methods

2.1 Materials

PVA of different grades (Gohsenol™ EG 05P and Gohsenol™ EG 18P, Nippon Gohsei, J) (PVA05 and PVA18); glycerol, GLY (Pharmagel, I); caffeine, CFF (A.c.e.f, I, melting point 238 °C).

2.2. Methods

2.2.1 Preparation of PVA-based formulations

Plasticized PVA formulations containing 15% by weight of GLY calculated on the dry polymer, indicated as PVA05GLY and PVA18GLY, were prepared by kneading. PVA powder, previously dried in an oven (40 °C for 24 h), was placed in a mortar and the liquid plasticizer was added dropwise under continuous mixing. The resulting mixture was oven dried at 40 °C for 8 h. Afterwards, aggregates were ground by means of a blade mill and the < 250 µm powder fraction was recovered. A tracer-containing formulation, indicated as PVA05GLY-CFF, was prepared immediately before processing by mixing in a mortar CFF powder, previously desiccated at 40 °C in an oven for 24 h, with PVA05GLY in a 1:9 weight ratio.

2.2.2 Manufacturing of PVA-based samples

Specimens having different geometries were prepared by HME and FDM. Virtual models of the straight bar (I-shape), U-shaped and helix items designed are reported in Figure 1.

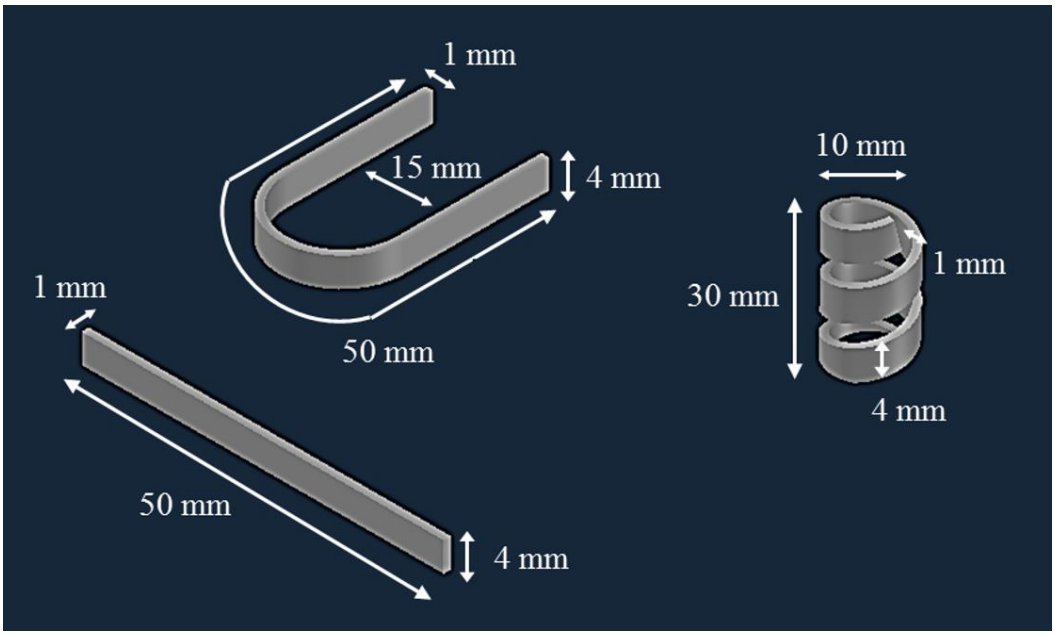

Figure 1: virtual models with dimensional details of items having original I-, U- and helix-shapes.

2.2.2.1 Extrusion

HME was performed by a twin-screw extruder (Haake™ MiniLab II, Thermo Scientific, US-WI) equipped with counter-rotating screws. The material was extruded through a rectangular cross-section die (4 x 1 mm). In Table 1, the polymeric formulations and processing conditions are reported. Both were selected through a preliminary setup based on evaluation of the product quality (*e.g.* aspect, homogeneity, compliance with previously set size specifications and reproducibility), taking advantage of the experience previously acquired on hot-processing of PVA (Melocchi et al., 2015b, 2016). Particularly, GLY was chosen as the plasticizer based on its widely reported use with PVA (Jang and Lee, 2003; Lin and Ku, 2008; Mohsin et al., 2011).

I-shaped samples of 50 mm in length were obtained by cutting. U- and helix-shape items required manual post-processing. In the former case, the material coming out of the extruder was bent around

a stainless steel tool (ø = 15 mm) and then removed after 2 min of cooling. In the latter case, the extruded material was wrapped around a stainless steel tool (ø = 6 mm), purposely developed with a groove of the helix to be obtained (distance between adjacent turns = 5 mm), and then removed after the same cooling time. Immediately after production, I-, U- and helix-shaped samples were packed in heat seal alufoil moisture barrier bags.

Filaments for FDM were prepared under analogous process conditions by extruding the same polymeric formulations through a custom-made aluminum circular die (ø = 1.80 mm), as reported in (Melocchi et al., 2016). Extruded rods were manually pulled and forced to pass through a caliper connected with the extruder and set at 1.80 mm. This was required to counteract possible swelling phenomena of the extruded rods and calibrate the relevant diameter, thus enhancing the yield of final product compliant with the specifications set, *i.e.* 1.75 ± 0.05 mm. After production and cooling, filament diameter was verified every 5 cm in length, and portions out of specifications were discarded. Indeed, filaments with diameter greater than 1.80 mm were unsuitable for printing.

2.2.2.2 3D printing

FDM was performed by a Kloner3D 240® Twin (Kloner3D, I) printer equipped with 0.4 mm nozzle (infill = 100%, layer height = 0.10 mm, printing speed = 23 mm/s, separation gap for raft and supports = 0.5 mm), using computer-aided design (CAD) files purposely developed. Items were designed using Autodesk® Autocad® 2016 software version 14.0 (Autodesk Inc., US-CA), saved in .stl format and imported to the 3D printer software (Simplify 3D, I). A further software (Netfab, I) was employed when the mesh number of the digital model needed to be increased, *i.e.* in the case of samples comprising curvatures.

Portions 25 cm long of the in-house prepared filaments were used. Printing temperature was set as reported in Table 1.

Table 1: HME and FDM process conditions

Material	HME			FDM
	T (°C)	Screw speed (rpm)	Torque (N·cm)	T (°C)
PVA05	200	100	190	200
PVA05GLY	170	100	100	180
PVA18GLY	200	100	220	n.d.*
PVA05GLY-CFF	175	100	120	185

*n.d. = not determined because of unfeasible manufacturing

2.2.3 Thermo-mechanical characterization

Samples cut from I-shaped items fabricated by HME and FDM, were subjected to differential scanning calorimetry (DSC) and dynamic-mechanical thermal analysis (DMTA).

DSC analyses were performed by DSC Q100 (TA Instruments, US-DE; n = 1), using nitrogen as a purge gas (70 mL/min). Indium was used as a calibration standard. Samples of about 10 mg were heated in aluminum crucibles from -50 °C to 240 °C, maintained at this temperature for 1 min, cooled down to -50 °C and reheated up to 240 °C. Both heating and cooling steps were run at 10 °C/min. Additional DSC tests were carried out with wet samples, maintained in distilled water for 30 min, and equilibrated under ambient conditions overnight (final water content of about 8-10% evaluated by thermogravimetric analysis).

DMTA tests were performed by a Q800 TA Instruments analyzer (TA Instruments, US-DE; n = 1), in displacement-controlled tensile mode, on ≈ 15 mm long specimens. The experiments were carried out at 1 Hz, with an applied displacement amplitude of 10 μm, from -50 °C to a maximum temperature equal to 100 °C / 120 °C, at a heating rate of 3 °C/min.

2.2.4 Water-induced shape memory experiments

The shape memory test consisted of two different phases, *i)* programming of the temporary shape and *ii)* recovery of the original shape (Figure 2). The programming step was performed as follows.

- Heating of the sample up to the deformation temperature ($T_{def} \approx T_g + 35$ °C, where T_g indicates the material glass transition temperature measured by DSC).

- Deformation, by means of specially designed tools, of the sample maintained at T_{def}. Samples having original U- or helix-shape were deformed to take on programmed temporary I-shape. Conversely, I-shaped samples were deformed to take on programmed temporary U-shape.

- Cooling of the sample in the fixed temporary shape below T_g. In case of plasticized PVAs, showing relatively low T_g, after deformation the samples were kept in a freezer at -20 °C in order to avoid early recovery.

Recovery of the original shape was obtained following immersion of the deformed samples into 100 mL of unstirred distilled water. The experiment was carried out both at room temperature and at 37 ± 0.5 °C, by using a thermoregulated bath. The recovery process was monitored using digital cameras (n = 1, Nikon D700 18-105 VR Kit, AF-S DX NIKKOR 18-105 mm f/3.5-5.6G ED VR, J and GoPro Hero Session, US-CA).

In case of originally I- or U- shaped samples, photographs acquired were processed by means of a specific software (ImageJ, US-MD) to measure the variation of the angle between the two arms (α) occurring during the recovery. Recovery index (RI) versus time curves were then built, with RI calculated as follows:

- for specimens with original I-shape

$$RI = \frac{\alpha - \alpha_p}{\pi - \alpha_p} \qquad \text{Eq. (1)}$$

- for specimens with original U-shape

$$RI = 1 - \frac{\alpha}{\alpha_p} \qquad \text{Eq. (2)}$$

where α_p is the angle obtained in the programming phase (angles in rad).

The time ($t_{RIfinal}$) to reach final RI (RI_{final}), *i.e.* the RI value calculated based on measurement after which no more changes in α were observed, was also recorded.

For specimens with original helix-shape, only the RI_{final} was considered, being calculated as follows:

$$RI_{final} = \frac{N_{fin}}{N_0} \qquad \text{Eq. (3)}$$

where N_{final} and N_0 represent the number of windings at the end of recovery and before programming, respectively.

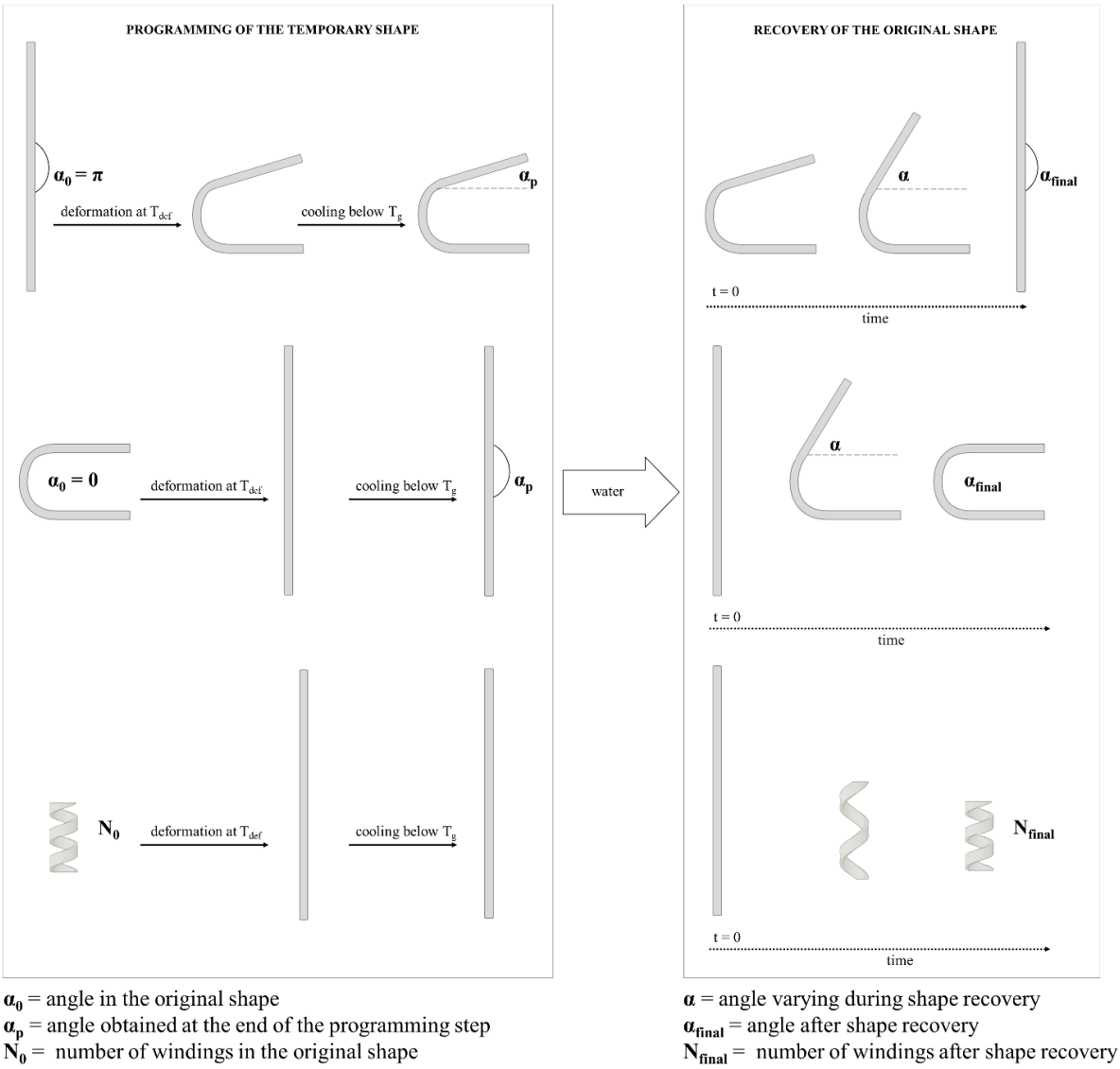

Figure 2: outline of the experiments performed to evaluate the water-induced shape memory response.

2.2.5 Evaluation of fluid uptake and residual dry mass

Extruded and printed samples having original I-shape (n = 3) were characterized in terms of fluid uptake and residual dry mass over 4 h of immersion in unstirred simulated urine fluid (400 mL) kept

at 37 ± 0.5 °C prepared as indicated in (Sherif et al., 2018). Each specimen was laid on a stainless steel net (w = 2.5 cm, h = 7 cm, mesh = 1.5 mm) before immersion and then withdrawn after predetermined time periods, gently blotted and weighed. Final dry masses were also determined after maintaining samples in an oven at 40 °C for 24 h. Two parameters were calculated, the percentage fluid uptake (FU) and the percentage residual dry mass (RDM), according to the following equations:

$$FU(\%) = \left[\frac{(W_m - W_d)}{W_m}\right] \times 100 \qquad \text{Eq. (4)}$$

where W_m is the mass of the wet sample on withdrawal and W_d is the mass of the sample after drying;

$$RDM(\%) = 1 - \left[\frac{(W_i - W_d)}{W_i}\right] \times 100 \qquad \text{Eq. (5)}$$

where W_i is the initial mass of the sample.

2.2.6 Evaluation of release performance

Tracer-containing extruded and printed samples were tested for release using a USP38 dissolution apparatus 2 (10 rpm, 37 ± 0.5 °C; Distek, CH; n = 3). 400 mL of simulated urinary fluid were used as the dissolution medium. Fluid samples were withdrawn at specific time points and assayed spectrophotometrically (λ = 206 nm). By linear interpolation of the release data immediately before and after the time point of interest, times to 10% and 90% release ($t_{10\%}$ and $t_{90\%}$, respectively) were calculated.

During the release test, photographs of samples were taken every 5 s (GoPro Hero Session, US-CA).

3. Results and Discussion

The temporary shape of a retentive intravesical delivery system should be such as to allow administration through a catheter without any constraints (*e.g.* straight bars with limited diameter and indefinite length). On the other hand, recovery of the original shape, designed to promote retention within the bladder for a pre-determined period of time (from few hours up to several days) without

damaging its walls, should spontaneously take place *in situ* as a result of interaction with biological fluids. If water soluble SMPs are chosen as main components of the delivery system, no invasive procedure would ultimately be needed for the relevant removal.

3.1 Design and fabrication of specimens

The experimental work was aimed at attaining specimens showing water-induced shape shifting phenomena representative of each stage of performance for the retentive intravesical delivery platform proposed. For this purpose, hot-processing techniques, namely HME and FDM, were employed. FDM has recently been demonstrated to be a versatile manufacturing process for fabrication of drug delivery systems having complex geometries and composition, such as orally administered dosage forms (*e.g.* tablets, matrices, capsules, hollow and multilayer systems), implants and inserts (Genina et al, 2017, Goole and Amighi, 2016, Goyanes et al., 2015, Maroni et al., 2017, Melocchi et al., 2015a, 2018, Okwuosa et al., 2017, Sandler and Preis, 2016, Tagami et al., 2018, Zema et al, 2016). In the particular field of intravesical delivery, which FDM has not been applied to so far, this 3D printing technique would grant the possibility of personalizing the pharmacological therapy in terms of type and dose of conveyed drugs, possible co-administration scheme (fixed drug combinations or extemporary compositions), and achievable release kinetics. With regard to HME, not only would it be viable for the device fabrication, but also is necessarily associated with FDM processing as it provides the filaments required for printer feeding.

Among polymers exhibiting water-induced shape memory response and good hot-processability, swellable/erodible ones, able to interact with aqueous fluids ultimately dissolving/eroding, appeared especially advantageous as main components for the delivery system. Indeed, such materials undergo a glass-rubber transition when in contact with biological fluids with formation of a gel, the dissolution/erosion behavior of which depends on the relevant viscosity and, therefore, on the polymer molecular weight. Particularly, PVA was selected based on both the experience gained on relevant processing *via* HME and FDM as well as the review of preliminary literature findings on the

exhibited water-driven shape memory ability, which relies on its semi-crystalline nature or may be obtained by crosslinking (De Jaeghere et al., 2015, Fang et al., 2017, Melocchi et al., 2015b, 2016, Qi et al., 2014). With respect to SMPs already proposed for drug delivery purposes, mainly including newly synthetized crosslinked polymers wanting regulatory approval, the PVA selected offers the advantage of a long-established use and safety profile (Nagahama et al., 2009, Neffe et al., 2009, Wischke et al, 2009, Wischke and Lendlein 2010). In addition, being available in different molecular weights, it was expected to be a versatile material that would allow for a range of diversified release rates of the active ingredient conveyed and bladder retention times of the system.

Different molecular weights of PVAs, either unplasticized or in admixture with a plasticizer and/or tracer, were used. In order to broaden the scope of information achievable in terms of process and performance, the specimens based on these formulations were conceived in three geometries, having different extent of complexity, either mimicking the original (*i.e.* enabling bladder retention) or the temporary (*i.e.* enabling administration) shape of the device: a U-shaped item, a helix, as a possible evolution of the U-shape, and a simple straight bar (I-shape). The latter shape was chosen as a prototypical screening tool on account of the expected ease of fabrication, while the helix shape was considered of particular interest in view of intravesical application as it combines several advantages and a rather simple design. As compared with the U-shape, helical geometry could not only take on a temporary bar-like shape suitable for administration and then recover the original retentive configuration, but also be expected to have improved bladder retention, thanks to their numerous windings, and enhanced patient compliance. Indeed, a helix might behave like a spring that undergoes compression from resting position and shortens its natural length, thereby withstanding possible mechanical stresses, deriving from muscle contraction during urination, and limiting discomfort. If further improvement of the helical geometry were pursued, the presence of any sharp tip might be overcome to reduce the potential for damaging the urothelium.

Originally I-, U- and helix-shaped samples were fabricated by FDM starting from in-house extruded filaments. Specimens having such designs were also fabricated by HME for comparison purposes and

were thus used as a reference to design the virtual models for FDM. By way of example, Figure 3 shows photographs of the extruded and printed samples based on plasticized PVA05. Notably, materials being extruded have to undergo bending and coiling before cooling to reach final original shapes other than straight ones, thus involving purposely-developed tools and attentive process design. Conversely, items having relatively complex geometries (*e.g.* U- and helix-shape) could directly be fabricated by 3D printing. Revision of CAD files was needed to counteract possible expansion phenomena encountered with the polymeric formulations in use following preliminary printing trials. Indeed, by calculating a correction coefficient, as described in (Melocchi et al, 2015a), printed items matching the dimensions of those prepared by HME were obtained. In addition, for samples comprising curvatures (*i.e.* originally U-shaped and helix-shaped specimens), the mesh number, *i.e.* a collection of vertices, edges and faces used to describe the shape of a tridimensional object, had to be increased in the virtual model in order to improve the resolution thus obtaining a smoother surface. FDM was performed by means of a 3D printer characterized by two arms working independently, which enabled contemporaneous fabrication of different parts thus reducing the overall printing time. The presence of a fixed build plate allowed to overcome manual calibration issues and also limited the exposure of the object in fabrication to uncontrolled airflow, known to hinder uniform cooling thereby impacting on product mechanical properties (*e.g.* reduced stiffness, layer detachment in the area subjected to greater cooling). Items were fabricated in the presence of a raft, because this turned out to increase adhesion of first printed layers to the build plate. Printing of helix-shaped items also required the use of supports between each winding to avoid collapsing during vertical growth. A separation gap of 0.5 mm was set between the object and the raft as well as supports to make them easily removable without damage. Printing speed was kept low (23 mm/s) to enhance accuracy and avoid dragging of latest layered material, which may cause detachment of the item in fabrication from the build plate. Under these conditions, PVA05-based formulations were successfully printed without technical issues at temperatures established on the basis of their thermal behavior. As expected, the presence of the plasticizer resulted in improved printing and reduced

number of failures. Notably, the obtained helical-samples, subjected to manual compression, were shown to behave like a spring, *i.e.* shorten in length when stressed and then return to the initial position after stress removal. In spite of the overall actions taken to make the process feasible, it was not possible to print any item starting from PVA18, either unplasticized or in admixture with GLY. Indeed, because the pressure needed for material extrusion during the 3D process is only exerted by the mass of the filament being loaded, the melt viscosity of such polymer was too high to enable its flow through the available nozzle. While increasing the printing temperature was expected to reduce the polymer viscosity, such an adjustment turned out not to be viable as browning of the material was observed. On the other hand, HME was successfully carried out with all the PVA formulations under investigation, except for PVA18 in the absence of plasticizer because torque values exceeding the maximum allowed by the equipment in use would have been needed.

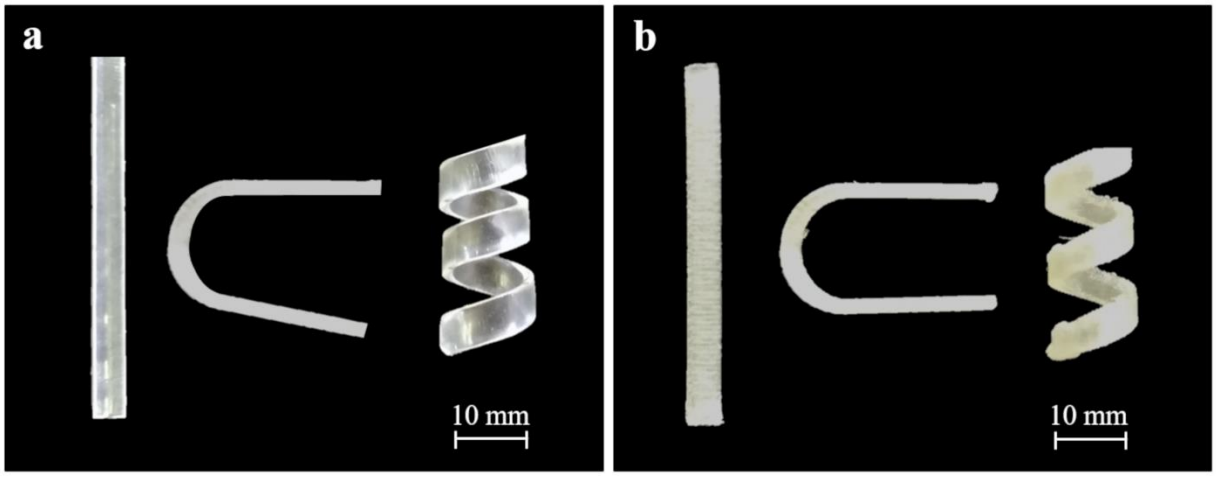

Figure 3: photographs of originally I-, U- and helix-shaped specimens based on PVA05GLY obtained by a) HME and b) FDM.

3.2 Shape memory response

A basic experimental screening was carried out on I-shaped specimens obtained by HME and FDM in order to determine how the thermo-mechanical properties of samples may lead to their shape memory. In particular, as the temperature required to activate the shape transformation strictly depends on the material glass transition temperature, DSC analyses were initially performed. Indeed,

shape shifting phenomena depend on amorphous regions of the polymer gaining mobility when T_g is reached, while permanent shape could be supported by crystalline domains, which would undergo melting at a higher temperature thus acting as net points (Fang et al, 2017). Therefore, evaluating how T_g is affected by the polymer grade, the presence of plasticizer and the interaction with water is of utmost importance because the temporary shape *i)* must be programmed at $T_{def} > T_g$ (in the present case $T_{def} \approx T_g + 35$ °C), *ii)* can be preserved keeping the material at $T < T_g$ and *iii)* is reversed to the original shape at $T > T_g$. In this specific case, shape recovery phenomena should take place at 37 °C. Because shape recovery is activated at temperatures above T_g, any change in such a property is expected to be highlighted in the shape memory experiments. By DMTA, the evolution of material stiffness was described, and in particular storage modulus was measured below room temperature (T_{room}) and at T_{def}, corresponding to sample stiffness before and after recovery, respectively.

3.2.1 DSC experiments

DSC thermograms are reported in Figure 4, choosing the second scan since it provided T_g values similar to those of the first one but easier to read. These curves displayed a regular shape, *i.e.* a well-defined inflection point corresponding to the material T_g, and no other exo-/endo-thermal signals. T_g values obtained from these thermograms are reported in Table 2: minor differences in T_g measured for extruded and printed specimens were observed.

The plasticization effect of GLY turned out evident for PVA05, as a decrease of 37 °C and 46 °C in T_g was noticed with PVA05GLY-based samples obtained by HME and FDM, respectively. Such an effect was attributed to the ability of the plasticizer to modify the 3D organization of the polymer matrix (Mohsin et al., 2011). In fact, due to its low-molecular weight and hydroxyl groups, GLY is known to lead to the formation of polymer-plasticizer hydrogen bonds to the detriment of interactions among polymer chains, thus reducing the intermolecular attraction forces and increasing the macromolecule mobility at temperatures below those at which the neat polymer undergoes transition.

In the case of wet samples, it was evident that also water taken up acted as a plasticizer for PVA, reasonably by weakening intra- and inter-molecular hydrogen bonds and increasing mobility of macromolecular chains (Figure 4a, Table 2). Indeed, progressive water absorption is known to concomitantly induce a decrease in the polymer T_g below room temperature until an equilibrium is reached. Particularly, the most marked decrease was recorded in the case of the wet as compared with dry PVA05 sample. The observed plasticization effect of water, allowing macromolecules to gain mobility, would enable activation of the shape shifting process at room temperature and below, which is the basis for the water-induced shape memory response.

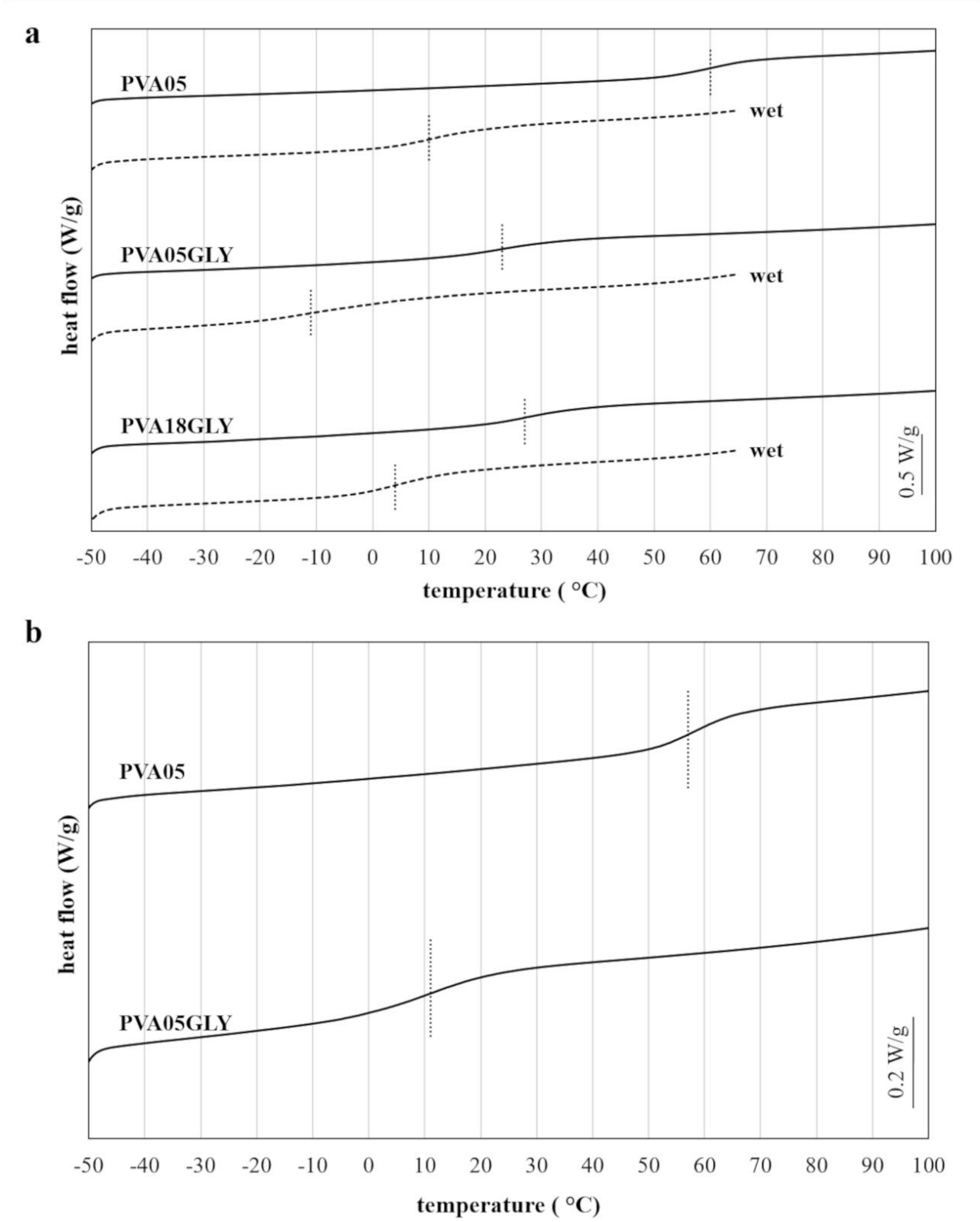

Figure 4: DSC thermograms (in the T_g region) from originally I-shaped specimens obtained by a) HME and b) FDM. Dotted vertical bars indicate T_g.

Table 2: T_g from DSC analyses, for originally I-shaped specimens obtained by HME and FDM. Data in brackets refer to wet samples

	T_g (°C)	
	HME	**FDM**
PVA05	60 (10)	57
PVA05GLY	23 (-11)	11
PVA18GLY	27 (4)	n.a.*

* n.a. = non-available sample because of unfeasible manufacturing

3.2.2 DMTA experiments

Figure 5 shows the storage modulus (E') *vs* temperature curves obtained from extruded and printed specimens subjected to DMTA.

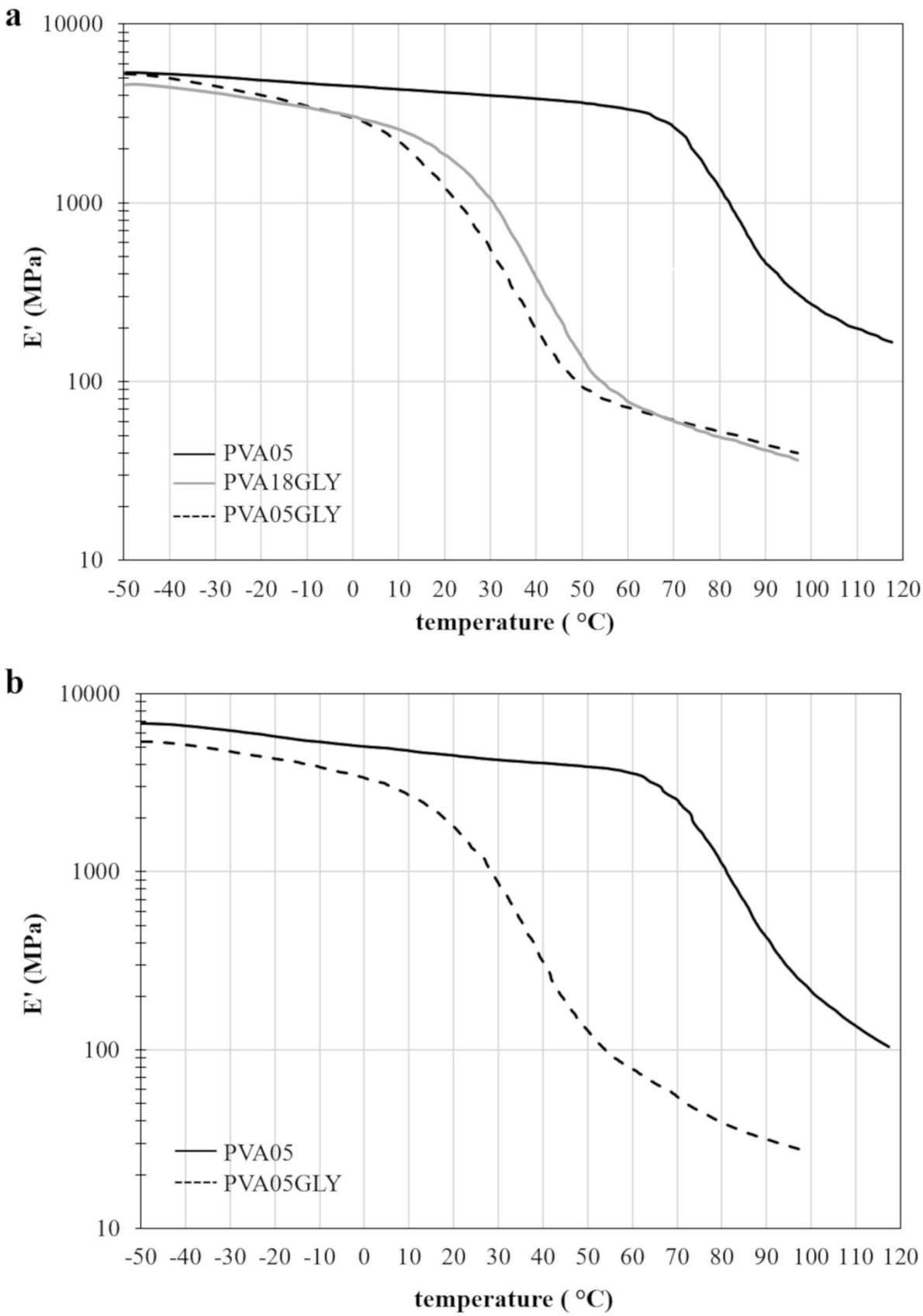

Figure 5: E' *vs* temperature curves from originally I-shaped specimens obtained by a) HME and b) FDM.

The plasticization effect induced by GLY, previously observed in DSC thermograms, was confirmed by DMTA data. Indeed, the reduced extent of interaction among PVA chains brought about by the addition of plasticizer resulted in a decrease in the sample stiffness, irrespective of the manufacturing technique considered. A decrease in T_g for GLY-containing specimens was confirmed by shifting of E' curves towards lower temperatures. E' traces also provided an indication of the stiffness of the material below and across the transition region. Table 3 reports E' values determined both at room temperature (E'_{Troom}) and at T_{def} (E'_{Tdef}), at which the material showed a rubbery behavior, as well as the relevant percentage difference (ΔE'), defined as:

$$\Delta E'(\%) = \frac{E'_{Troom} - E'_{Tdef}}{E'_{Troom}} \times 100 \qquad \text{Eq. (6)}$$

These values were chosen since E'_{Troom} would be representative of the stiffness of samples in their original shape, E'_{Tdef} would be an estimation of such a characteristic right after the shape memory transition, while ΔE' would represent the overall stiffness change during the transition. E'_{Tdef} and ΔE' may overestimate and underestimate, respectively, stiffness and overall change in stiffness, since it is known that water absorption, and eventually polymer dissolution, would lead to a relevant decrease.

Table 3: E'_{Troom}, E'_{Tdef} and ΔE' from originally I-shaped specimens obtained by HME and FDM

	E'_{Troom} (MPa)		**E'_{Tdef} (MPa)**		**ΔE' (%)**	
	HME	**FDM**	**HME**	**FDM**	**HME**	**FDM**
PVA05	4060	4330	440	410	89	90
PVA05GLY	830	2750	70	120	92	96
PVA18GLY	1420	n.a.*	80	n.a.*	94	n.a.*

* n.a. = non-available sample because of unfeasible manufacturing

Irrespective of the manufacturing technique employed, PVA05 specimens displayed a stiff behavior at T_{room}, the storage modulus decreasing of one order of magnitude at T_{def} with an overall stiffness change of about 90%. Not only the PVA05GLY but also PVA18GLY samples exhibited, because of the presence of GLY, lower E'_{Troom} and E'_{Tdef}, and a slightly higher overall variation (92-96%). The

higher stiffness shown at T_{room} by printed specimens with respect to extruded ones might be ascribed to processing.

In general, the drop of E' indicates the occurrence of a relaxation process that, for these materials, could be ascribed to glass transition of PVA (Chartoff et al, 2009). In support of the DSC data, T_g was also evaluated by DMTA, confirming minor differences, associated with the technique employed for sample manufacturing, as observed by DSC. Indeed, for a given material and specimen preparation method, a difference between transition temperatures determined by DSC and by DMTA, with the latter being systematically higher than the former, is expected and intrinsically related to the differences between the two experimental techniques and corresponding testing parameters, such as heating rate and frequency. Because transition temperatures coming from DMTA exhibit testing frequency dependence, T_g values obtained by DSC were used for assessment of T_{def} in the shape memory experiments.

3.2.3 Shape recovery experiments

The water-induced shape recovery process was studied in unstirred distilled water at room temperature, by monitoring evolution of the shape of extruded and printed samples from the temporary one. By analyzing photographs taken at successive time points, RI was calculated to describe the shape recovery process. By way of example, images of printed PVA05GLY specimens having different original shapes are collected in Table 4.

Table 4: photographs acquired during shape recovery experiments (room temperature) of PVA05GLY specimens having original I- and U-shape obtained by FDM. A solid line is superimposed to highlight the recovery process

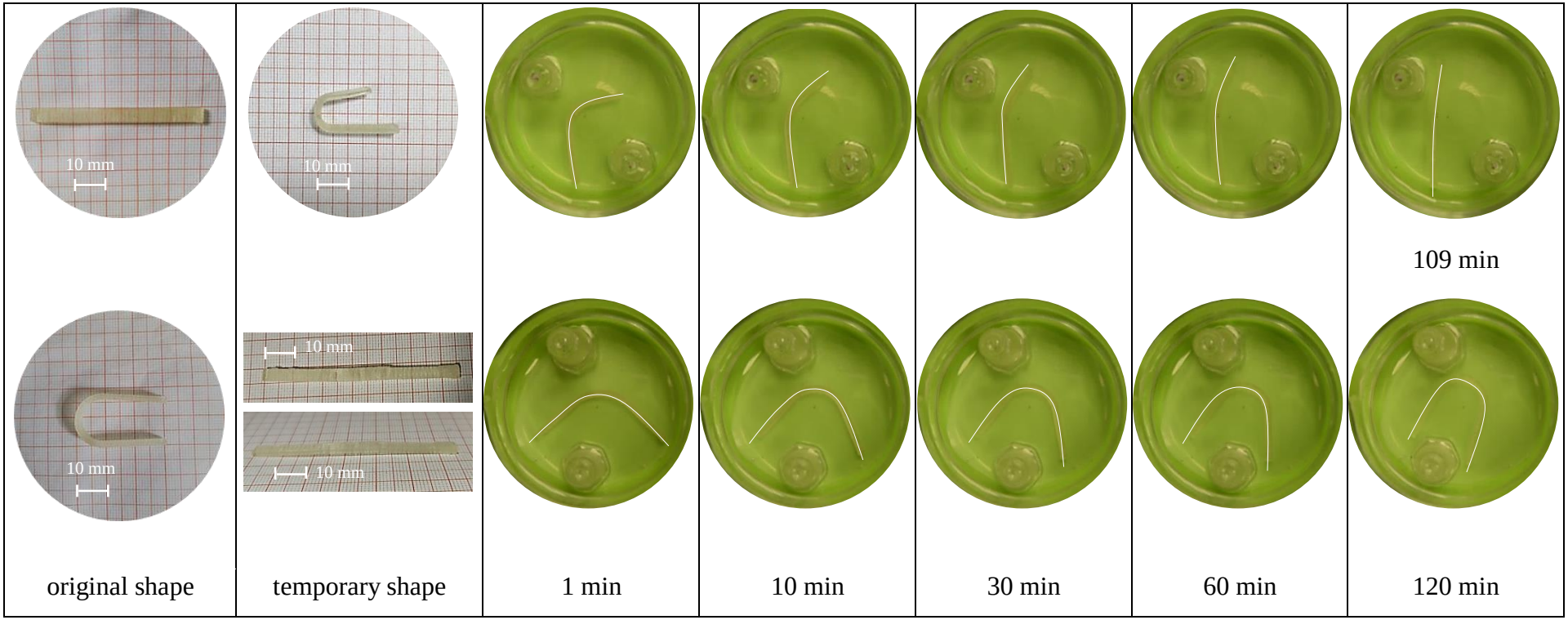

The recovery ability observed for a very simple original shape (*i.e.* I-shaped specimen programmed to take on temporary U-shape) was also shown by samples having an original U-shape (programmed to take on temporary I-shape) and comparable recovery times were found in both cases, irrespective of geometry. A shape-shifting effect similar to that exhibited by printed PVA05GLY samples was observed for the other formulations examined. An almost full recovery of the original shape was obtained from specimens having all geometries under investigation. The recovery process was also monitored over time and α was measured at successive time points to calculate the corresponding RI values. Recovery curves from selected extruded and printed samples with different original shapes are reported in Figure 6. With PVA05 samples, determination of RI in the final stage of the recovery process was impaired by concurrent polymer dissolution causing distortion of the specimens, which impaired the assessment of their shape evolution. In such cases, measurements had to be interrupted, and this was highlighted in the curves by marking the last RI value acquired.

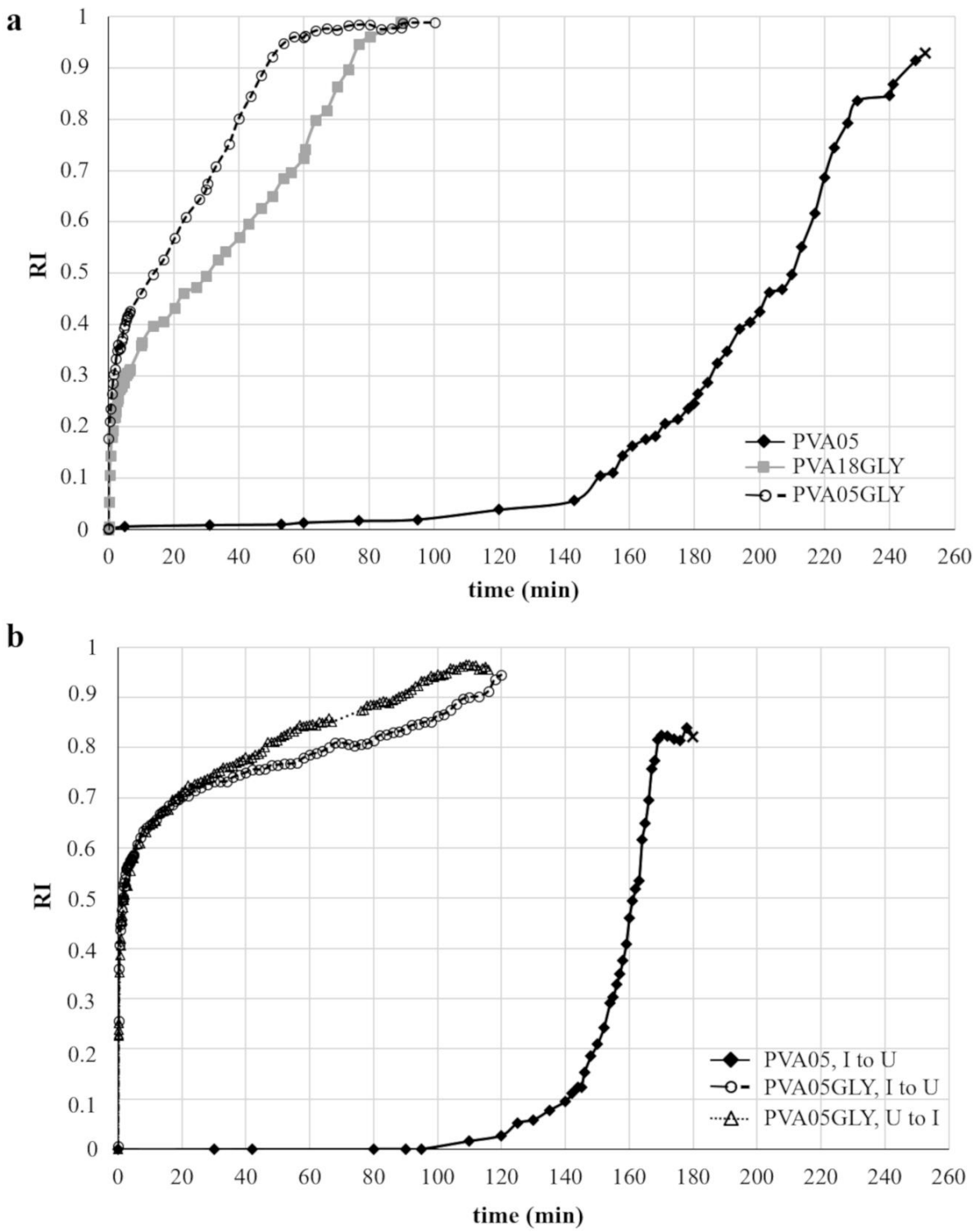

Figure 6: RI *vs* time curves from a) originally I-shaped specimens of all compositions obtained by HME and b) originally I- and U-shaped PVA05-based specimens obtained by FDM, tested at room temperature (x indicates the last datum acquired before measurements were impaired by the polymer dissolving).

For samples manufactured by HME, the addition of GLY to PVA05 modified the recovery process kinetics (Figure 6a). This is consistent with previous reports showing the effect of plasticizer on the shape memory response of semi-crystalline polymers (Cai et al., 2017). With unplasticized PVA05, recovery showed an initial induction phase followed by a high rate phase (about 120 min long). By contrast, with PVA05GLY the process started with a high rate without any induction phase and the overall duration of recovery was reduced. These differences may be related to the fact that for PVA05GLY, having T_g below the recovery test temperature, the recovery process would be a combination of water- and temperature-induced shape memory effects, whereas for the unplasticized polymer, having T_g above the test temperature of approximately 30 ° C, recovery would result from water-induced shape memory only. Moreover, because of the greater free volume associated with the lower T_g, water diffusion phenomenon may be faster with the plasticized polymer, thus resulting in a faster activation of the shape memory effect. As regards PVA18, HME was feasible with the formulation containing GLY only, and the resulting sample exhibited a similar recovery pattern as compared with the PVA05GLY one, although the rate of the process was lower after the first few minutes of testing. The influence of molecular weight of the polymer on the relevant shape shifting phenomena would deserve further investigation, also considering literature findings mainly focused on its impact on recovery index (Chen et al., 2007, Petisco-Ferrero et al., 2016).

In Figure 6b, it can be observed that the recovery curve of the printed PVA05 specimen showed an analogous induction phase, of approximately 2 h, with respect to the extruded sample having the same composition. However, the recovery rate in the subsequent phase turned out higher for the specimen obtained by FDM. The printed *vs* extruded PVA05GLY specimens were characterized by much faster initial recovery followed by a decrease in the process rate after some minutes from the beginning of the test, regardless of their original shape. Such differences in the initial recovery rate might be related to the different surface porosity/roughness of specimens fabricated by HME and FDM. Although specimens of comparable dimensions were prepared by the two techniques, the effective surface/volume ratio that governs water absorption kinetics is likely to be higher for printed than

extruded specimens due to a more porous structure resulting from the additive manufacturing process. The subsequent decrease in recovery rate of printed items, together with a less marked difference in the time needed for complete recovery observed with plasticized *vs* unplasticized samples, may be suggestive of the inherent layered nature, which would be brought out by the contact with water. It could be hypothesized that the various layers may not swell jointly following progressive water penetration. By contrast, extruded items would most likely be expected to behave as a continuous matrix. However, such an aspect is little known and is worth being explored, because in-depth studies comparing the water-induced shape memory response of extruded and printed items have not been reported in the scientific literature. An investigation into the possible differences in the temperature-induced shape memory behavior of items obtained starting from poly(ethylene-co-methacrylic acid) either by FDM or compression molding, a technique well-known for producing non-porous items, has so far been reported (Zhao et al., 2017).

Recovery studies were also carried out under body temperature conditions. Table 5 summarizes RI_{final} values obtained and corresponding $t_{RIfinal}$, collected at room temperature and 37 °C from extruded and printed specimens having original I-shape.

Table 5: RI_{final} values and corresponding $t_{RIfinal}$ from specimens having original I-shape tested at room temperature and 37 °C

		Room temperature		**37 °C**	
		RI_{final}	$t_{RIfinal}$ (min)	RI_{final}	$t_{RIfinal}$ (min)
HME	PVA05	0.93[a]	251[a]	0.97	146
	PVA05GLY	0.99	100	0.86	28
	PVA18GLY	0.99[a]	90[a]	0.92[a]	55[a]
FDM	PVA05	0.82[a]	180[a]	n.d.	n.d.
	PVA05GLY	0.97	109	0.88[a]	26[a]

[a] determination hindered by dissolving of the polymer with possible distortion of the specimen
n.d. = not determined because of pronounced distortion of the specimen

Generally high RI_{final} was shown by both extruded and printed specimens, with lower values for PVA05-based formulations. Because shape recovery and polymer dissolution occur concomitantly,

RI_{final} could hardly be determined when the rate of shape recovery was lower than that of dissolution, thus leading to considerably reduced size or changes in consistency of the sample. In the case of the printed PVA05 specimen, it was not even possible to determine RI_{final} because of dissolution-driven distortion that was ascribed to the reduced gel viscosity and sample stiffness due to the high extent of hydration reached, close to the dissolution threshold. At both temperatures, the presence of GLY accelerated the recovery process, with up to a four-fold decrease in $t_{RIfinal}$ at 37 °C for PVA05GLY specimens. Because the T_g was by far lower than the test temperature, such a marked acceleration of recovery may have resulted from a combination of water- and temperature-induced shape memory effects. A reduction of $t_{RIfinal}$ was observed for all formulations tested at 37 °C as compared with room temperature, with extent of reduction of $t_{RIfinal}$ consistent with that of T_g values, as could be expected based on the increased mobility of the amorphous PVA domains. In the case of extruded specimens containing plasticizer (PVA05GLY and PVA18GLY), the time needed for recovery turned out to be affected by the polymer molecular weight at 37 °C.

The overall results confirmed that the use of originally straight bar-shaped samples as a screening tool could be appropriate, and the information gathered may profitably be exploited in the design of devices with more complex geometries

3.3 Fluid uptake and residual dry mass

Because thermo-mechanical properties and recovery of the original shape of samples was demonstrated to be affected not only by temperature but also by their exposure to aqueous media, it was deemed interesting to investigate the kinetics of biological fluid uptake. Concomitantly, the mass loss behavior of the same specimens was studied over time. Indeed, the overall bladder retention time of the device, the onset and time frame of shape shifting phenomena as well as its ability to control the release of the conveyed drug would be related to the rate and extent of hydration and erosion/dissolution of the polymeric formulation.

Extruded and printed specimens having original I-shape were thus evaluated for FU and RDM, employing simulated urinary fluid kept at 37 ± 0.5 °C to mimic the environment in which the system was supposed to perform.

From FU and RDM profiles, reported in Figure 7, it turned out evident that the rate of fluid uptake was by far higher than that of mass loss. Indeed, approximately 40% of fluid taken up was reached within the first 15 min of testing, irrespective of the formulation and manufacturing technique considered. In the case of extruded items, the rate of mass loss of PVA05GLY was greater than that of PVA18GLY specimens. This could be explained on the basis of the different molecular weights of the employed polymer, which is known to be associated with viscosity of the hydrated matrix thus affecting the relevant rate of erosion/dissolution. The addition of GLY to PVA05 slightly accelerated the initial fluid uptake, which was evident especially in the case of extruded samples reasonably due to their less porous structure that could have hindered penetration of the aqueous medium. Because of pronounced hygroscopicity, the plasticizer may have increased water affinity of specimens, thus favoring absorption of the aqueous fluid (Mohsin et al., 2011). Indeed, the hydroxyl groups of GLY would be able to establish hydrogen bonds with both water and polymer, thus increasing the molecular mobility of the latter and the free volume in the samples. In the case of PVA05, the threshold absorbed amount of aqueous medium needed for sufficient mobility of the polymer chains to be acquired and dissolution to take place was therefore higher than with the plasticized formulation. Interestingly, the fluid uptake behavior of the specimens was consistent with the shape recovery previously discussed. As expected, activation of shape shifting phenomena in GLY-containing samples was especially rapid because the polymer T_g was not only decreased by the presence of plasticizer but also by the relatively high extent of fluid taken up in the first minutes of testing.

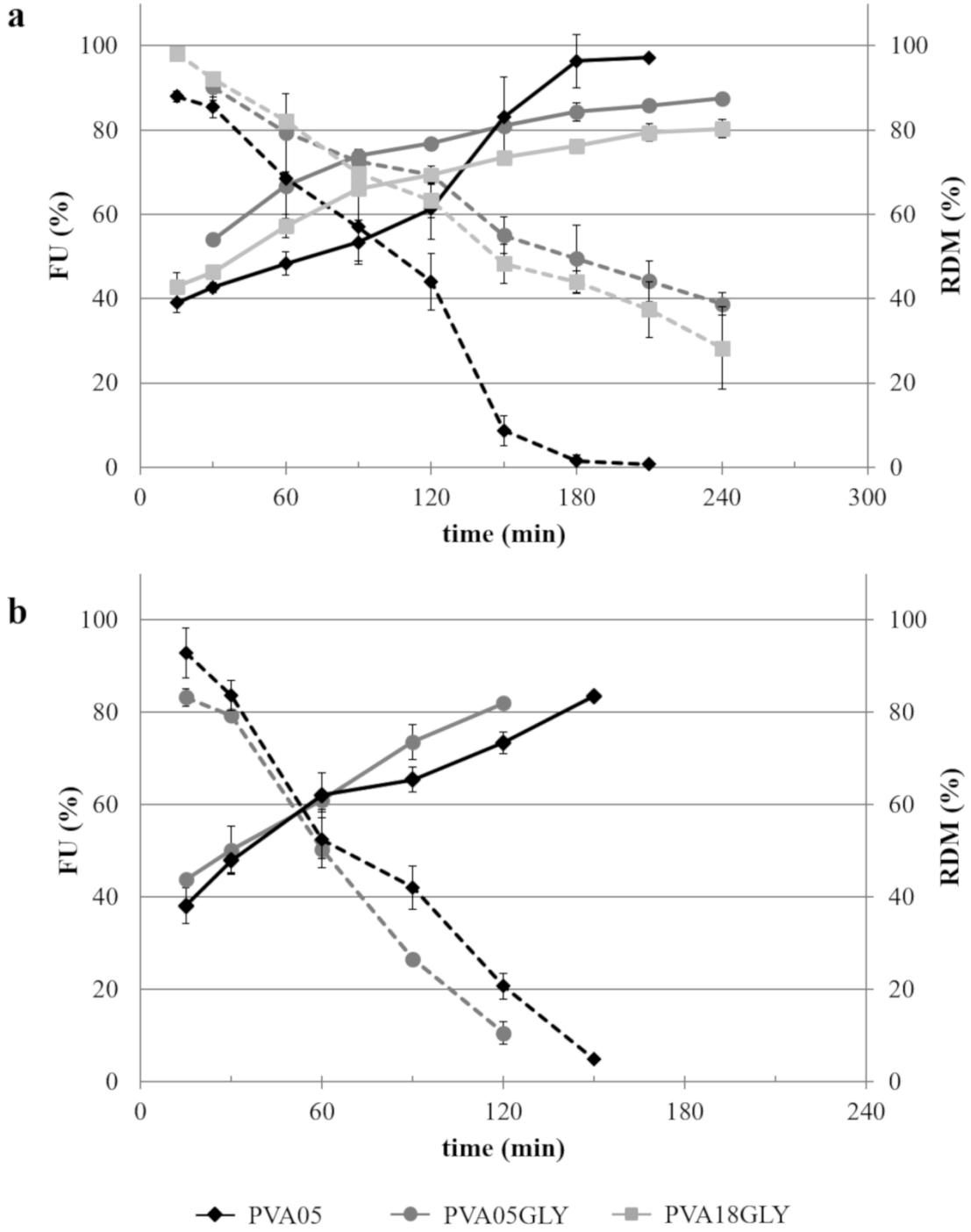

Figure 7: average FU (solid lines) and RDM (dashed lines) curves from originally I-shaped specimens obtained by a) HME and b) FDM.

3.4 Evaluation of tracer-containing specimens

The potential of the PVA-based formulations under investigation for slowly releasing an active ingredient while undergoing prompt shape modifications was preliminarily evaluated using

specimens containing CFF as an analytical tracer. Specimens having original I-shape were initially characterized for thermo-mechanical properties. A further decrease in T_g was found with respect to the corresponding samples devoid of CFF (T_g = 1 °C *vs* T_g = -3 °C for extruded *vs* printed items), which was already observed with a different thermoplastic polymer (Burgess et al., 2015). Moreover, the printed and extruded tracer-containing specimens showed comparable stiffness at T_{room} while higher values of E'_{Tdef}, thus resulting in an overall stiffness reduction of about 70% (E'_{Troom} = 1110 MPa *vs* E'_{Troom} = 1010 MPa and E'_{Tdef} = 340 *vs* E'_{Tdef} = 280 MPa for extruded *vs* printed items). Samples having different original shapes, fabricated *via* both techniques, showed the ability to undergo shape recovery induced by water at room temperature and 37 °C, regardless of the presence of CFF (Table 6 and 7). With originally I-shaped samples, recovery turned out faster with respect to the previously tested ones, which was consistent with the T_g values relevant to the PVA05GLY-CFF formulation. In spite of a comparable extent of recovery, $t_{RIfinal}$ was nearly doubled for the extruded specimen as compared with the printed one. This was in agreement with the findings obtained from tracer-free specimens and is not surprising on account of the layered nature of items attained by additive manufacturing.

Table 6: RI_{final} values and corresponding $t_{RIfinal}$ from specimens having original I- and helix-shape tested at room temperature

	Original shape	**RI_{final}**	**$t_{RIfinal}$ (min)**
HME	I-shape	0.94	40
	helix-shape	0.75	26
FDM	I-shape	0.76[a]	12[a]
	helix-shape	0.71	12

[a] determination hindered by dissolving of the polymer with possible distortion of the specimen

Table 7: photographs acquired during shape recovery experiments (37 °C) of PVA05GLY-CFF specimens having original helix shape, obtained by HME and FDM, programmed to take on a temporary I-shape. A solid line is superimposed to highlight the recovery process

HME	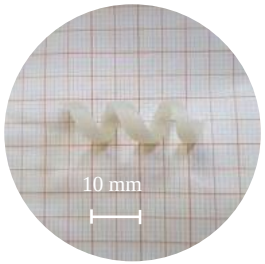					
FDM	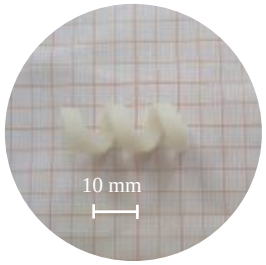					
	original shape	1 min	5 min	10 min	15 min	30 min

Release of the tracer from extruded and printed samples having original I-shape was studied after programming and fixing of the temporary U-shape, in order to evaluate the performance during recovery (Figure 8a). For this purpose, photographs of specimens were collected throughout the release test, and selected images relevant to printed items are reported in Figure 8b by way of example.

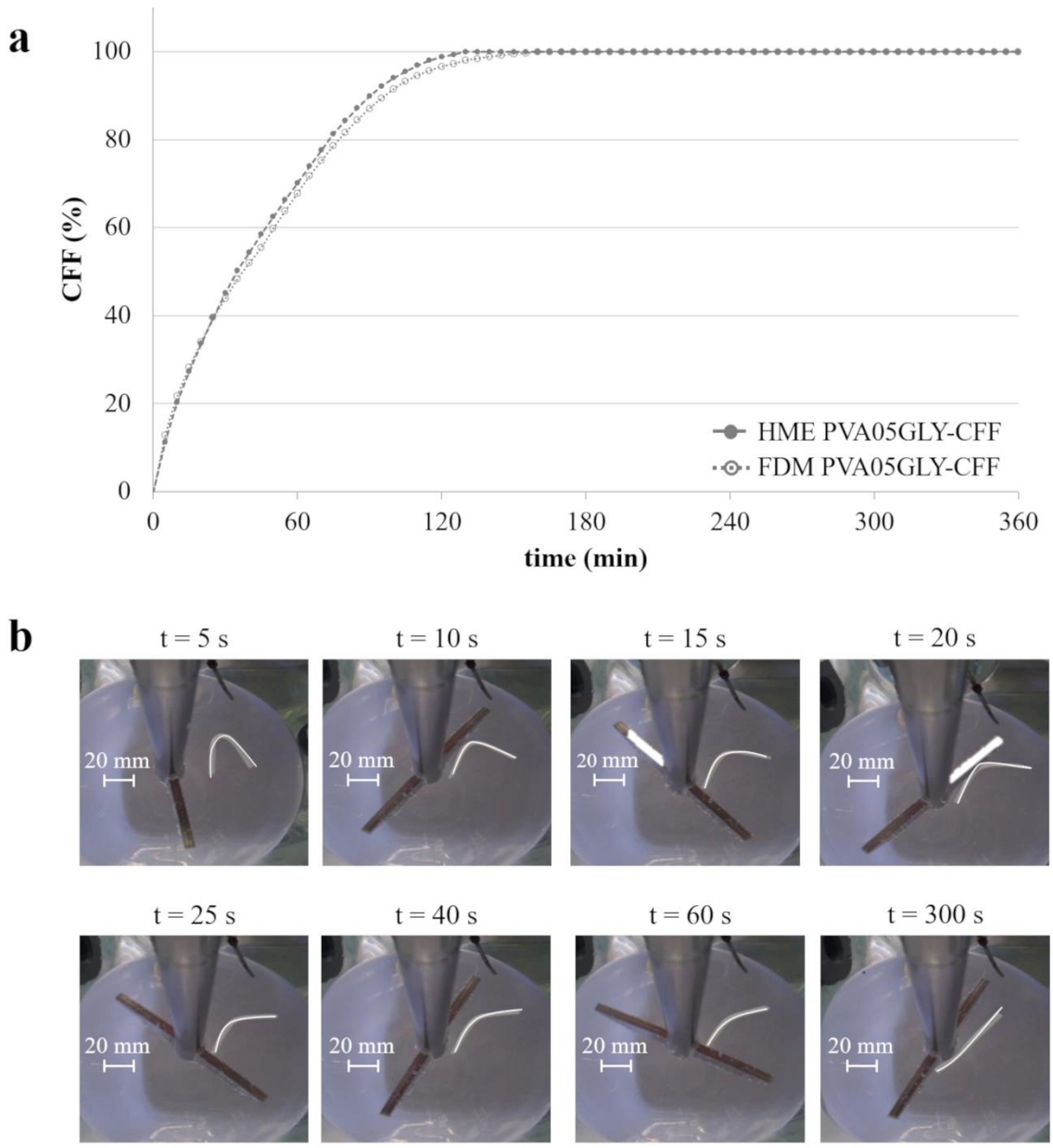

Figure 8: a) release profiles from originally I-shaped PVA05GLY-CFF specimens obtained by HME and FDM following programming and fixing of the temporary U-shape and b) photographs of the printed specimen at successive time points during the test. A solid line is superimposed to highlight the recovery process.

Release curves from extruded and printed specimens were almost superimposed. The release started without any lag phase and was completed within 2 h. Notably, with both extruded and printed specimens, the original straight shape was almost fully recovered before $t_{10\%}$, the most marked changes occurring within 60 s.

Conclusions

Indwelling drug delivery systems could be highly beneficial in the treatment of bladder diseases by increasing the intravesical residence time of drugs and compensating for the relevant washout. Such systems would thereby overcome failures and discomfort connected with repeated instillations through catheters. Moreover, they would allow different release kinetics to be established. The use of SMPs, in view of their ability to take on a programmed/temporary shape and recover the permanent/original one in the presence of an external *stimulus*, was regarded as an innovative strategy to develop retentive drug delivery systems with convenient administration mode. Among swellable/erodible SMPs characterized by water-induced shape memory response and good melt-processability, PVA of pharmaceutical-grade was selected for design and fabrication *via* hot-processing techniques, namely FDM 3D printing and HME, of an indwelling device for intravesical drug administration involving no removal procedure. In this respect, application of a 3D printing technique to an SMP would notably provide the basis for 4D printing because of the programmed changes in shape of the printed item occurring over time.

Starting from formulations based on PVA of different molecular weights, specimens having diverse original shapes and compositions were successfully extruded and printed. After programming and fixing of a temporary shape, these exhibited the desired ability to recover the original one following interaction with aqueous fluids, and the overall recovery as well as its rate were consistent with those expected according to the thermo-mechanical properties of the investigated materials. The recovery process was relatively fast, particularly at 37 °C, which was considered potentially advantageous in the prospect of achieving prompt retention of the final system immediately after insertion into the

bladder. The softening upon glass-rubber transition of the polymer would impart favorable hardness characteristics to the device, such that limited mechanical impact on the bladder epithelium could be ensured. Purposely fabricated samples containing an analytical tracer turned out able to modify the release of the latter before complete dissolution, yielding prolonged release patterns consistent with the molecular weight of PVA employed. Thus, multi-functionality of the PVA-based materials investigated was highlighted, entailing water-induced shape shifting, controlled release of a tracer and erosion/dissolution in biological fluids. More extended and varied release profiles, associated with diversified retention times, could be pursued by appropriate formulation and processing choices, such as selection and combination of polymers having higher molecular weights, modulation of the amount of plasticizer, addition of release modifiers and improvement of the equipment to ease processing.

Although preliminary in scope, this study pointed out the viability of the proposed approach based on hot-processing of a pharmaceutical-grade polymer having water-induced shape memory response in the manufacturing of retentive intravesical delivery systems, opening up new perspectives in application of 4D printing to the pharmaceutical field.

References

M. Behl, A. Lendlein Shape memory polymers, Mater. Today 10 (2007) 20-28. https://doi.org/10.1016/S1369-7021(07)70047-0.

S.K. Burgess, J.S. Lee, C.R. Mubarak, R.M. Kriegel, W.J. Koros, Caffeine antiplasticization of amorphous poly(ethylene terephthalate): Effects on gas transport, thermal, and mechanical properties, Polymer 65 (2015) 34-44. https://doi.org/10.1016/j.polymer.2015.03.051.

S. Cai, Y.-C. Sun, J. Ren, H.E. Naguib, Toward the low actuation temperature of flexible shape memory polymer composites with room temperature deformability via induced plasticizing effect, J. Mater. Chem. B 5 (2017) 8845-8853. https://doi.org/10.1039/C7TB02068F.

B.Q.Y. Chan, Z.W.K. Low, S.J.W. Heng, S.Y. Chan, C. Owh, X.J. Loh, Recent advances in shape memory soft materials for biomedical applications, ACS Appl. Mater. Interfaces 8 (2016) 10070-10087. https://doi.org/10.1021/acsami.6b01295.

R.P. Chartoff, J.D. Menczel, S.H. Dillman, Dynamic Mechanical Analysis (DMA), in: J.D. Menczel, R.B. Prime (Eds.), Thermal Analysis of Polymers: fundamentals and applications, Hoboken: John Wiley & Sons; 2009.

S. Chen, J. Hu, Y. Liu, H. Liem, Y. Zhu, Q. Meng, Effect of molecular weight on shape memory behavior in polyurethane films, Polym. Int. 56 (2007) 1128-1134. https://doi.org/10.1002/pi.2248.

M.J. Cima, H. Lee, K. Daniel, L.M. Tanenbauma, A. Mantzavinou, K.C. Spencer, Q. Ong, J.C. Sy, J.Jr. Santini, C.M. Schoellhammer, D. Blankschtein, R.S. Langer, Single compartment drug delivery, J. Control. Release 190 (2014) 157-171. https://doi.org/10.1016/j.jconrel.2014.04.049.

W. De Jaeghere, T. De Beer, J. Van Bocxlaer, J.P. Remon, C. Vervaet, Hot- melt extrusion of polyvinyl alcohol for oral immediate release applications, Int. J. Pharm. 492 (2015) 1-9. https://doi.org/10.1016/j.ijpharm.2015.07.009.

Z. Ding, C. Yuan, X. Peng, T. Wang, H.J. Qi, M.L. Dunn, Direct 4D printing via active composite materials, Sciences Adv. 3 (2017) e1602890-e1602896. https://doi.org/10.1126/sciadv.1602890.

E.F. El Feninat, G. Laroche, M. Fiset, D. Mantovani, Shape memory materials for biomedical applications, Adv. Eng. Mater. 4 (2002) 91-104. https://doi.org/10.1002/1527-2648(200203)4:3<91:AID-ADEM91>3.0.CO;2-B.

Z.Q. Fang, Y.D. Kuang, P.P. Zhou, S.Y. Ming, P.H. Zhu, Y. Liu, H.L. Ning, G. Chen, Programmable shape recovery process of water-responsive shape memory poly(vinyl alcohol) by wettability contrast strategy, ACS Appl. Mater. Interfaces 9 (2017) 5495-5502. https://doi.org/10.1021/acsami.6b14868.

O.C. Farokhzad, J.D. Dimitrakov, J.M. Karp, A. Khademhosseini, M.R. Freeman, R. Langer, Drug delivery systems in urology - getting “smarter”, Urol. 68 (2006) 463-469. https://doi.org/10.1016/j.urology.2006.03.069.

B. Gao, Q. Yang, X. Zhao, G. Jin, Y. Ma, F. Xu, 4D bioprinting for biomedical applications, Trends Biotechnol. 34 (2016) 746-756. https://doi.org/10.1016/j.tibtech.2016.03.004.

N. Genina, J.P. Boetker, S. Colombo, N. Harmankaya, J. Rantanen, A. Bohr, Anti-tuberculosis drug combination for controlled oral delivery using 3D printed compartmental dosage forms: from drug product design to in vivo testing, J. Control. Release 268 (2017) 40-48. https://doi.org/10.1016/j.jconrel.2017.10.003.

J. Goole, K. Amighi, 3D printing in pharmaceutics: A new tool for designing customized drug delivery systems, Int. J. Pharm. 499 (2016) 376-394. https://doi.org/10.1016/.ijpharm.2015.12.071.

A. Goyanes, J. Wang, A. Buanz, R. Martínez-Pacheco, R. Telford, S. Gaisford, A.W. Basit, 3D Printing of medicines: engineering novel oral devices with unique design and drug release characteristics, Mol. Pharm. 12 (2015) 4077-4084. https://doi.org/10.1021/acs.molpharmaceut.5b00510.

S. GuhaSarkar, R. Banerjee, Intravesical drug delivery: challenges, current status, opportunities and novel strategies, J. Control. Release 148 (2010) 147-159. https://doi.org/10.1016/j.jconrel.2010.08.031.

M. D. Hager, S. Bode, C. Weber, U S. Schubert, Shape memory polymers: Past, present and future developments, Prog. Polym. Sci. 49-50 (2015) 3-33. https://doi.org/10.1016/j.progpolymsci.2015.04.002.

W. M. Huang, Z. Ding, C. C. Wang, J. Wei, Y. Zhao, H. Purnawali, Shape memory materials, Mater. Today 13 (2010) 54-61. https://doi.org/10.1016/S1369-7021(10)70128-0.

C.-C. Hsu, Y.-C. Chuang, M.B. Chancellor, Intravesical drug delivery for dysfunctional bladder, Int. J. Urol. 20 (2013) 552-562. https://doi.org/10.1111/iju.12085.

J. Jang, D. K. Lee, Plasticizer effect on the melting and crystallization behavior of polyvinyl alcohol, Polymer 44 (2003) 8139-8146. https://doi.org/10.1016/j.polymer.2003.10.015.

E.A. Klausner, E. Lavy, M. Friedman, A. Hoffman, Expandable gastroretentive dosage forms, J. Control. Release 90 (2003) 143-162. https://doi.org/10.1016/S0168-3659(03)00203-7.

A.Y. Lee, J. An, C.K. Chua, Two-way 4D printing: a review on the reversibility of 3D-printed shape memory materials, Eng. 3 (2017) 663-674. https://doi.org/10.1016/J.ENG.2017.05.014.

H. Lee, M.J. Cima, An intravesical device for the sustained delivery of lidocaine to the bladder, J. Control. Release 149 (2011) 133-139. https://doi.org/10.1016/j.jconrel.2010.10.016.

S.H. Lee, Y.B. Choy, Implantable devices for sustained, intravesical drug delivery, Int. Neurourol. J. 20 (2016) 101-106. https://doi.org/10.5213/inj.1632664.332.

A. Lendlein, M. Behl, B. Hiebl, C. Wischke. Shape-memory polymers as a technology platform for biomedical applications, Expert Rev. Med. Devices 7 (2010) 357-379. https://doi.org/10.1586/erd.10.8.

A. Lendlein, R. Langer, Biodegradable, elastic shape-memory polymers for potential biomedical applications, Science 296 (2002) 1673-1676. https://doi.org/10.1126/science.1066102.

C.-A. Lin, T.-H. Ku, Shear and elongational flow properties of thermoplastic polyvinyl alcohol melts with different plasticizer contents and degrees of polymerization, J. Mater. Process Technol. 200 (2008) 331-338. https://doi.org/10.1016/j.jmatprotec.2007.08.057.

C. Liu, H. Qin, P.T. Mather, Review of progress in shape-memory polymers, J. Mater. Chem. 17 (2007) 1543-1558. https://doi.org/10.1039/b615954k.

A. Maroni, A. Melocchi, F. Parietti, A. Foppoli, L. Zema, A. Gazzaniga, 3D printed multi-compartment capsular devices for two-pulse oral drug delivery, J. Control. Release 268 (2017) 10-18. https://doi.org/10.1016/j.jconrel.2017.10.008.

A. Melocchi, F. Parietti, G. Loreti, A. Maroni, A. Gazzaniga, L. Zema, 3D printing by fused deposition modeling (FDM) of a swellable/erodible capsular device for oral pulsatile release of drugs, J, Drug Deliv. Sci. Technol. 30 Part B (2015a) 360-367. https://doi.org/10.1016/j.jddst.2015.07.016.

A. Melocchi, G. Loreti, M.D. Del Curto, Maroni A., A. Gazzaniga, L. Zema, Evaluation of hot- melt extrusion and injection molding for continuous manufacturing of immediate-release tablets, J. Pharm. Sci. 104 (2015b) 1971-1980. https://doi.org/10.1002/jps.24419.

A. Melocchi, F. Parietti, A. Maroni, A. Foppoli, A. Gazzaniga, L. Zema, Hot-melt extruded filaments based on pharma-grade polymers for 3D printing by fused deposition modeling, Int. J. Pharm. 509 (2016) 255-263. https://doi.org/10.1016/j.ijpharm.2016.05.036.

A. Melocchi, F. Parietti, S. Maccagnan, M.A. Ortenzi, S. Antenucci, F. Briatico-Vangosa, A. Maroni, A. Gazzaniga, L. Zema, Industrial development of a 3D-printed nutraceutical delivery platform in the form of a multicompartment HPC capsule, AAPS PharmSciTech. (2018). https://doi.org/10.1208/s12249-018-1029-9.

M. Maniruzzamann (Ed.), 3D and 4D printing in biomedical applications: process engineering and additive manufacturing, Weinheim: Wiley VCH; 2018.

M. Mohsin, A Hossin, Y. Haik, Thermal and mechanical properties of poly(vinyl alcohol) plasticized with glycerol, J. Appl. Polym. Sci. 122 (2011) 3102-3109. https://doi.org/10.1002/app.34229.

K. Nagahama, Y. Ueda, T. Ouchi, Y. Ohya, Biodegradable shape-memory polymers exhibiting sharp thermal transitions and controlled drug release, Biomacromolecules 10 (2009) 1789-1794. https://doi.org/10.1021/bm9002078.

A.T. Neffe, B.D. Hanh, S. Steuer, A. Lendlein, Polymer networks combining controlled drug release, biodegradation, and shape memory capability, Adv. Mater. 21 (2009) 3394-3398. https://doi.org/10.1002/adma.200802333.

J.C. Nickel, P. Jain, N. Shore, J. Anderson, D. Giesing, H. Lee, G. Kim, K. Daniel, S. White, C. Larrivee-Elkins, J. Lekstrom-Himes, M. Cima, Continuous intravesical lidocaine treatment for interstitial cystitis/bladder pain syndrome: safety and efficacy of a new drug delivery device, Sci. Transl. Med. 4 (2012) 1-11. https://doi.org/10.1126/scitranslmed.3003804.

J. Nirmal, Y.-C. Chuang, P. Tyagi, M.B. Chancellor, Intravesical therapy for lower urinary tract symptoms, Urol. Sci. 23 (2010) 70-77. https://doi.org/10.1016/j.urols.2012.07.005.

T.C. Okwuosa, B.C. Pereira, B. Arafat, M. Cieszynska, A. Isreb, M.A. Alhnan, Fabricating a shell-core delayed release tablet using dual FDM 3D printing for patient-centred therapy, Pharm. Res. 34 (2017) 427-437. https://doi.org/10.1007/s11095-016-2073-3.

S. Petisco-Ferrero, J. Fernández, M.M. Fernández San Martín, P.A. Santamaría Ibarburu, J.R. Sarasua Oiz, The relevance of molecular weight in the design of amorphous biodegradable polymers with optimized shape memory effect, J. Mech. Behav. Biomed. Mater. 61 (2016) 541-553. https://doi.org/10.1016/j.jmbbm.2016.04.027.

X.D. Qi, X.L. Yao, S. Deng, T.N. Zhou, Q. Fu, Water-induced shape memory effect of graphene oxide reinforced polyvinyl alcohol nanocomposites, J. Mater. Chem. A Mater. 2 (2014) 2240-2249. https://doi.org/10.1039/C3TA14340F.

N. Sandler, M. Preis, Printed drug-delivery systems for improved patient treatment, Trends Pharmacol. Sci. 37 (2016) 1070-1080. https://doi.org/10.1016/j.tips.2017.01.002.

A.Y. Sherif, G.M. Mahrou, F.K. Alanazi, Novel in-situ gel for intravesical administration of ketorolac, Saudi Pharm. J. 26 (2018) 845-851. https://doi.org/10.1016/j.jsps.2018.03.014.

W. Sokolowski, A. Metcalfe, S. Hayashi, L. Yahia, J. Raymond, Medical applications of shape memory polymers, Biomed. Mater. 2 (2007) S23-S27. https://doi.org/10.1088/1748-6041/2/1/S04.

T. Tagami, N. Nagata, N. Hayashi, E. Ogawa, K. Fukushige, N. Sakai, T. Ozeki, Defined drug release from 3D-printed composite tablets consisting of drug loaded polyvinylalcohol and a water-soluble or water-insoluble polymer filler, Int. J. Pharm. 543 (2018) 361-367. https://doi.org/10.1016/j.ijpharm.2018.03.057.

I.S. Tobias, H. Lee, G.C.Jr. Engelmayr, D. Macaya, C.J. Bettinger, M.J. Cima, Zero-order controlled release of ciprofloxacin-HCl from a reservoir-based, bioresorbable and elastomeric device, J. Control. Release 146 (2010) 356-362. https://doi.org/10.1016/j.jconrel.2010.05.036.

P. Tyagi, M. Kashyap, H. Hensley, N. Yoshimura, Advances in intravesical therapy for urinary tract disorders, Expert Opin. Drug Deliv. 13 (2016) 71-84. https://doi.org/10.1517/17425247.2016.1100166.

C. Wischke, A. Lendlein, Shape-memory polymers as drug carriers -a multifunctional system, Pharm. Res. 27 (2010) 527-529. https://doi.org/10.1007/s11095-010-0062-5.

C. Wischke, T.A. Neffe, S. Steuer, A. Lendlein, Evaluation of a degradable shape-memory polymer network as matrix for controlled drug release, J. Control. Release 138 (2009) 246-250. https://doi.org/10.1016/j.jconrel.2009.05.027.

L. Yahia, Shape memory polymers for biomedical applications, Woodhead Publishing, London, 2015

B. Yang, W.M. Huang, C. Li, C.M. Lee, L. Li, On the effects of moisture in a polyurethane shape memory polymer, Smart Mater. Struct. 13 (2004) 191-195. https://doi.org/10.1088/0964-1726/13/1/022.

M.M. Zacchè, S. Srikrishna, L. Cardozo, Novel targeted bladder drug-delivery systems: a review, Res. Rep. Urol. 7 (2015) 169-178, https://doi.org/10.2147/RRU.S56168.

Z. Zhao, F. Peng, K.A. Cavicchi, M. Cakmak, R.A. Weiss, B.D. Vogt, Three-dimensional printed shape memory objects based on an olefin ionomer of zinc-neutralized poly(ethylene-co-methacrylic acid), ACS Appl. Mater. Interfaces. 9 (2017) 27239-27249. https://doi.org/10.1021/acsami.7b07816.

L. Zema, A. Melocchi, A. Maroni, A. Gazzaniga, 3D printing of medicinal products and the challenge of personalized medicine, J. Pharm. Sci. 106 (2016) 1697-1705. https://doi.org/10.1016/j.xphs.2017.03.021.

***Conflict of Interest**

Declaration of interests

☒ The authors declare that they have no known competing financial interests or personal relationships that could have appeared to influence the work reported in this paper.

☐The authors declare the following financial interests/personal relationships which may be considered as potential competing interests:

IJP AUTHOR CHECKLIST

Dear Author,

It frequently happens that on receipt of an article for publication, we find that certain elements of the manuscript, or related information, is missing. This is regrettable of course since it means there will be a delay in processing the article while we obtain the missing details.

In order to avoid such delays in the publication of your article, if accepted, could you please run through the list of items below and make sure you have completed the items.

Overall Manuscript Details

- Is this the final revised version? X
- Are all text pages present? X
- Are the corresponding author's postal address, telephone and fax numbers complete on the manuscript? X
- **Have you provided the corresponding author's e-mail address?** X
- **Manuscript type – please check one of the following:**
  - Full-length article X
  - Review article ☐
  - Rapid Communication ☐
  - Note ☐
  - Letter to the Editor ☐
  - Other ☐
- **Manuscript section – paper to be published in:**
  - Pharmaceutical Nanotechnology section ☐
  - Personalised Medicine section ☐

Manuscript elements

- Short summary/abstract enclosed? X
- 3-6 Keywords enclosed? X
- Complete reference list enclosed? X
- Is the reference list in the correct journal style? X
- Are all references cited in the text present in the reference list? X
- Are all **original** figures cited in the text enclosed? X
  Electronic artwork format? ----------
- Are figure legends supplied? X
- Are all figures numbered and orientation provided? X
- Are any figures to be printed in colour? ☐
  If yes, please list which figures here:----------
- If applicable, are you prepared to pay for reproduction in colour? ☐
- Are all tables cited in the text supplied? X

General

- Can you accept pdf proofs sent via e-mail? X